논문 2012-49TC-5-5

송신 배열 안테나의 경로 보정과 비선형 보상의 결합 기술

(A Technique Combining the Path Calibration and Nonlinear Compensation in a Transmitting Antenna Array System)

임 선 민*, 김 민**, 은 창 수***

(Sunmin Lim, Min Kim, and Changsoo Eun)

요 약

본 논문에서는 스마트 안테나 시스템에 대해 경로 결함들의 보정과 전력 증폭기의 비선형성 보상을 결합하는 새로운 기술을 제안하였다. 배열 안테나의 각각의 경로들이 동일한 특성을 갖기 위한 보정과 보상을 위해 선형 항에 3차 항을 추가한 다항식과 간접 학습 구조를 사용하였다. 본 논문에서는 컴퓨터 모의실험을 통해 성능을 입증하였다. 모의실험 결과, 단 하나의 3차 항을 추가하여 선형 결함들뿐만 아니라 모든 비선형 효과까지 효율적으로 보상함을 확인하였다.

Abstract

We propose a new scheme combining the calibration of the path imperfections and the compensation of HPA nonlinearity in the downlink OFDM smart antenna systems. We use a two term third-order polynomial (without second-order term) and the indirect learning architecture for calibration and compensation, to make each path of the antenna array have equal characteristics. We test our scheme with computer simulations. The result shows that, with the addition of only one third-order term, the adverse nonlinear effects as well as the those of linear imperfections can be effectively compensated.

Keywords : Smart antenna, array antenna system, indirect learning architecture, calibration, compensation.

Ⅰ. Introduction

The smart antennas have recently emerged as a means to improve the performance of mobile radio systems. The smart antenna is an antenna array system combined with space-time signal processing. For the beamforming, which is one of the most fundamental space-time processing techniques, accurate estimations of DOA (direction of arrivals) and time delay are essential. Most high-resolution DOA estimation algorithms, however, assume the ideal matches between array signal paths and linear amplification, which is usually not the case in practice. The gain and phase responses of each signal path vary due to temperature and humidity changes, mismatches of cable lengths, and cross-talks arising from mutual couplings[1]. Moreover, the nonlinearity in the high-power amplifiers makes the overall system performance worse. Various array calibration methods with or without known source direction have been proposed[2~4]. However, these methods only calibrate linear imperfections of signal paths with the assumption of perfectly linear power amplifications. Usually, the linear amplification means an inefficient

* 정회원, 한국전자통신연구원 (ETRI)
** 학생회원, 충남대학교 전자전파정보통신공학과 (Chungnam National University)
*** 평생회원-교신저자, 충남대학교 (Chungnam National University)
접수일자: 2012년3월23일, 수정완료일: 2012년5월12일

power amplifier that operates at a power lever back off the saturation region. If the nonlinearity compensation can be combined with the calibration process, an efficient smart antenna may be attained.

We propose a new technique that combines the calibration and the compensation. With the addition of only one filter coefficient for each signal path, we can attain both the calibration and the nonlinearity compensation. We calibrate and compensate the signal paths one-by-one using one training block. Since the calibration and compensation (cal-com) should be performed before the signal is put onto each path, the training block is placed forward of each signal path, which necessitates the use of indirect learning architecture.

This paper is organized as follows. In section Ⅱ, we briefly discuss the path imperfections that arise in the antenna array systems. In section Ⅲ, we describe the indirect learning algorithm used to train the cal-com block. In section Ⅳ, we propose a scheme for training the cal-com block for the overall system operation. In section Ⅴ, we show simulation results to verify the performance of the proposed scheme. In section Ⅵ, we conclude our work.

Ⅱ. The path Imperfections of Antenna Array System

The imperfections arising in the smart antenna system can be divided into two categories: linear and nonlinear. The linear imperfections are the mutual coupling which arises when the paths are closely placed, the length discrepancy of cables or conductors which connect each path to the antennas, and the channel imbalances attributed to the component errors and the local changes of temperature, humidity, vibration and so on[1]. The nonlinear imperfections originate from the nonlinear devices such as mixers and high power amplifiers. The nonlinear effect of mixers is usually negligible since it is removed by filters. In this paper, we consider the downlink system only for brevity. However, the generality of the proposed scheme is not lost and can be extended to the uplink case as well[1, 5].

Mutual coupling is a typical linear imperfection. Two paths in proximity place influence on each other. This interaction is called mutual coupling. It changes the current on each path. If we neglect the noise, the mutual coupling can be taken into account as

$$\mathbf{x}[n] = \mathbf{Y}_0 \mathbf{A}(\theta)\mathbf{s}[n] \tag{1}$$

where $\mathbf{x}[n]$ is $M \times 1$ snapshot vector of the signal current components in the paths, $\mathbf{Y}_0$ is $M \times M$ normalized admittance matrix, $\mathbf{A}(\theta)$ is $M \times L$ steering matrix, $\mathbf{s}[n]$ is $L \times 1$ source voltage vector, and M is the number of the antenna elements.

The length discrepancy of the cables or conductors that carry each signals introduces imbalance of phase shifts and losses. If we assume the transmission lines are loss-free, they cause phase imbalance only. The phase imbalance can be taken into account as

$$\mathbf{x}[n] = \mathbf{L}\mathbf{A}(\theta)\mathbf{s}[n] \tag{2}$$

where

$$\mathbf{L} = \mathrm{diag}(e^{-j2\pi \triangle z_i/\lambda}),\ i = 1, ..., M \tag{3}$$

is the matrix that represents the phase imbalance and $\triangle z_i$ are the differences in the length of the transmission lines.

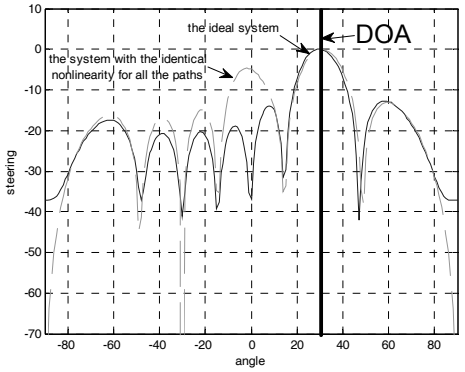

그림 1. 이상적인 시스템과 모든 경로가 동일한 비선형성을 가진 배열 안테나 시스템의 빔 패턴 비교

Fig. 1. Comparison of beam patterns of the ideal system, with that a system when the nonlinearity of all the paths are identical.

The gain and phase imbalance in the transmit trains arises by both the antenna elements themselves and the related electronics, i.e., the variance of component values, antenna mismatches, and the local variations of temperature, humidity, etc. The path imbalance can be taken into account as

$$\mathbf{x}[n] = \mathbf{G}\mathbf{A}(\theta)\mathbf{s}[n] \tag{4}$$

where the imbalance matrix $\mathbf{G}$ is defined by

$$\mathbf{G} = \mathrm{diag}(g_i e^{-j\phi_i}), i = 1, ..., M \tag{5}$$

where g_i is the gain and ϕ_i is the phase for transmit train i.

Previously published calibration methods attempted to compensate for linear imperfection only. When these methods are applied to the antenna array that has both linear and nonlinear imperfections, only the linear effects are calibrated, leaving the nonlinearity uncompensated. Let us assume a situation where an identical nonlinearity exists in all the paths of the antenna array. The Fig. 1 shows the beam pattern when linear imperfections do not exist and the common nonlinearity in all the paths is given by

$$y[n] = a_1 x[n] + a_3 x^3[n] \tag{6}$$

where $a_0 = 0.7 + 0.25i$, $a_1 = 0.1529 + 0.1i$. The DOA is assumed 30°. The solid line is the case without nonlinearity and the dotted line is the case with nonlinearity. We observe that, though the main beam is formed to the right direction, a second beam is generated to the wrong direction. Moreover, the constellation shown in Fig. 2 reveals that the nonlinearity introduced the phase rotation and constellation miss-alignment. From the result, we assert that, when there is nonlinearity, the existing calibration methods do not deliver adequate correction, which leaves room for improvement through the compensation of the nonlinearity. When the nonlinearity in each path is different from each other, even the main beam formation can not be guaranteed. We will add only one more nonlinear term to the calibration to mitigate all the adverse effects arising from the nonlinearity.

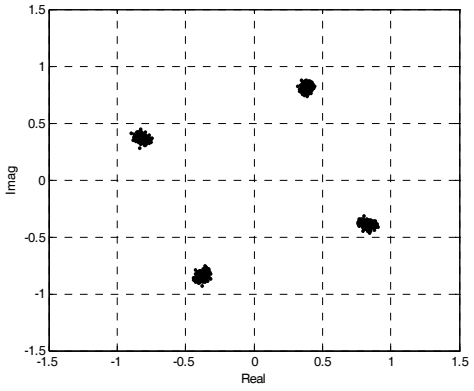

그림 2. 모든 경로가 동일한 비선형성을 가진 배열 안테나 시스템의 성상도

Fig. 2. Signal constellation of the antenna array system when the nonlinearity of all the paths are identical.

Each signal path in the antenna array can be represented as Fig. 3. The signal is converted into the analog signal by a D/A converter, then converted to an RF signal by an up converter. The RF signal is transmitted through a high power amplifier and antenna. Since the cal-com is performed in the baseband, the proposed method should be applied before the signal is put into the D/A converter.

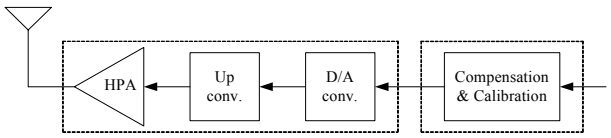

그림 3. 다운링크에서 각각의 신호 경로에 대한 보정과 보상

Fig. 3. Calibration and compensation for each signal path in dowlink.

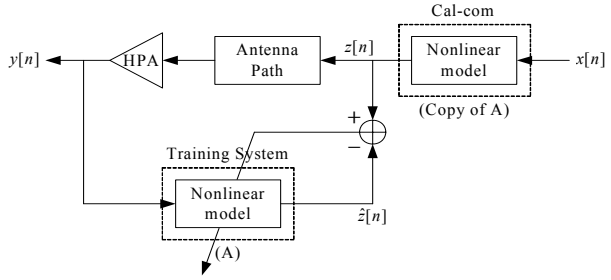

그림 4. 간접 학습 구조

Fig. 4. The indirect learning architecture.

Ⅲ. The path Imperfections of Antenna Array System

Fig. 4 shows the indirect learning architecture that is used for cal-com. The feedback path labeled 'Training System' (block A) is a third order polynomial (without the second-order term) system with $y[n]$ as its input and $\hat{z}[n]$as its output. The actual cal-com operation is performed by the cal-com block which is the exact copy of the training block. The cal-com block has $x[n]$ as its input and $z[n]$ as its output. Ideally, we would like to have $y[n]=x[n]$, which renders $z[n]=\hat{z}[n]$ and the error $e[n]=0$. Given $y[n]$ and $z[n]$, we will find the parameters of block A which make the error energy $\| e[n] \|^2$ minimum. The error energy is expressed as

$$\| e[n] \|^2 = \| z[n]-\hat{z}[n] \|^2 \tag{7}$$

Since the linear imperfections are memoryless, we use a polynomial as the cal-com block (and training block as well). Despite that we calibrate the linear imperfections and compensate for the HPA nonlinearity altogether, we need only one more term and adopt readily the VSS-LMS (variable step size least mean square) algorithm[7][8] for the polynomial coefficient adaptation. The VSS-LMS is known to have a faster convergence characteristic than LMS. A third-order polynomial is represented by

$$p[n]=h_1 x[n]+h_3 x[n]|x[n]|^2 \ . \tag{8}$$

The update rule for the coefficients is given by

$$\mathbf{h}[n+1]=\mathbf{h}[n]+\mu[n]e[n]\mathbf{x}[n] \tag{9}$$

where $\mathbf{h}[n]$ is the vector whose elements are the coefficients of a third order polynomial, which is represented by

$$\mathbf{h}=[h_1, h_2] \tag{10}$$

and $\mathbf{x}[n]$ is the input signal plus the third-order term represented by

$$\mathbf{x}[n]=[x[n], x[n]|x[n]|^2] \tag{11}$$

and $\mu[n]$ is the variable step size, which is given by

$$\mu[n+1]=\alpha\mu[n]+\gamma e^2[n] \tag{12}$$

where α, γ are suitable constants which determine the update amount.

Ⅳ. The proposed method combining calibration and compensation

Fig. 5 shows the whole antenna array system with the proposed cal-com and training blocks utilizing the indirect learning architecture. We use a polynomial as the nonlinear systems for cal-com. The training block, shown in the dotted box between the switches A and B, is used commonly by all paths turn-by-turn by the switches A and B. Once the switches select a path, the training block updates the contents of the corresponding cal-com block in the path using the indirect learning algorithm.

Here we assume that the nonlinear characteristic of the HPA changes slowly with time: the changes in the nonlinear system characteristics are mostly due to the temperature drift, aging, etc., which have long time constants. Once the adaptation algorithm has converged, the new set of filter coefficients is

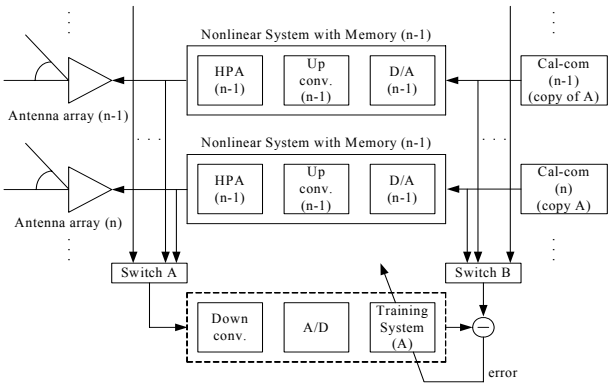

그림 5. 전체 배열 안테나 시스템의 경로 보정과 비선형성 보상

Fig. 5. The path calibration and nonlinearity compensation in the whole antenna array system.

plugged into the corresponding cal-com block. Since the characteristics of the system changes slowly, the setup in Fig. 5 can be run intermittently: i.e., we may run the training block only when a new adaptation is needed.

Ⅴ. Computer simulation

We verify the performance of the proposed scheme through computer simulations. As the test signal, we used a mobile WiMax signal. The bandwidth of the mobile WiMax signal is 8.75 MHz, the sampling frequency is 10 MHz, the sub-carrier spacing is 9.76 kHz, and FFT size is 1024. Table 1 shows the antenna system parameters used in the simulation. The simulations were carried out for an array of eight, center-fed dipole antennas which are linearly spaced by the half a wavelength. Effective power matching was assumed, which means the load impedance values were set to the conjugate of antenna impedance values. Tables 2-4 show the antenna array imperfections used in the simulations[1].

표 1. 모의실험에 사용된 배열 안테나 시스템의 파라미터
Table 1. System parameters used in the simulations.

Parameter	Value
Array geometry	Uniform linear antenna array
Inter-element spacing	1/2 λ
Carrier frequency	2.3 GHz
Number of antennas	8
DOA	30°

표 2. 상호 결합에 의한 상호 임피던스
Table 2. The mutual impedances due to the mutual coupling.

$d_r = d/\lambda$	$Z_{MC}(\Omega)$
0	$74+42i$
0.5	$-12+29i$
1	$4+18i$
1.5	$-3-11i$
2	$1+10i$
2.5	$-1-7i$
3	0
3.5	0

Table 2 shows the mutual impedances attributed to mutual coupling. The first column represents the relative spacing $d_r = d/\lambda$ for each paths and second column is the corresponding mutual impedances. The mutual impedance for $d_r = 0$ means the self impedance. Since the load impedance is $Z_L = 74 - i42$, the mutual coupling is expressed as

$$\mathbf{Y}_0 = \mathbf{Z}_0^{-1} = \begin{bmatrix} 1+\frac{Z_{11}}{Z_L} & \cdots & \frac{Z_{1M}}{Z_L} \\ \vdots & \ddots & \vdots \\ \frac{Z_{M1}}{Z_L} & \cdots & 1+\frac{Z_{MM}}{Z_L} \end{bmatrix} \tag{13}$$

where $\mathbf{Z}_0$ is the normalized impedance matrix.

Table 3 shows the phase shifts due to the cable length discrepancy that are randomly distributed within 10% of λ.

Table 4 shows the gain and phase of the each

표 3. 케이블 길이 차이에 따른 위상 천이
Table 3. The phase shifts due to the cable length differences.

Path	The cable length differences
1	$e^{i1.3835}$
2	$e^{i1.3891}$
3	$e^{i1.3862}$
4	$e^{i1.4157}$
5	$e^{i1.4782}$
6	$e^{i1.4396}$
7	$e^{i1.5213}$
8	$e^{i1.5526}$

표 4. 신호 경로의 이득과 위상
Table 4. The gains and phases of the signal paths.

Path	The gain and phase
1	1
2	$0.9762e^{i0.0346}$
3	$0.9362e^{i0.0743}$
4	$1.0247e^{i0.1239}$
5	$1.0142e^{-i0.0891}$
6	$1.0763e^{i0.0245}$
7	$0.9874e^{-i0.1362}$
8	$0.9988e^{-i0.1187}$

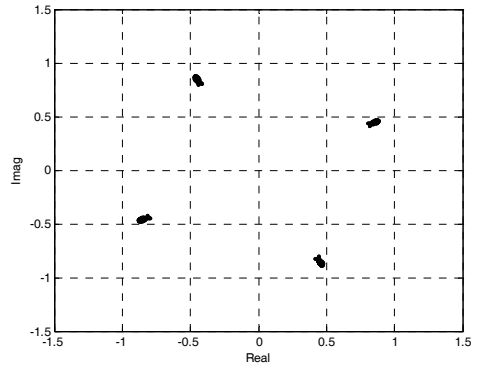

(a) QPSK

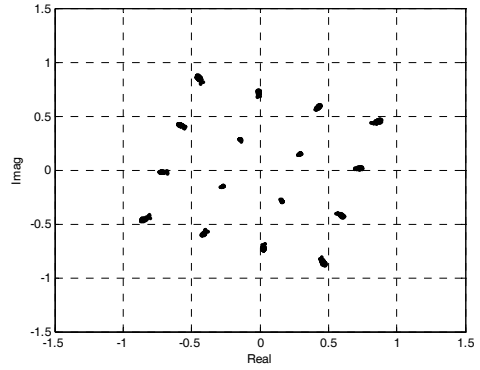

(b) 16-QAM

그림 6. 선형 결함을 가진 배열 안테나 시스템의 신호 성상도

Fig. 6. Signal constellations of the antenna array system with linear imperfections.

signal path that are randomly distributed within 10% of the gain and phase.

We compare the constellation of the signals and the beam pattern without calibration with ideal ones for the imperfections described so far on the assumption that the HPAs are all identical and linear. Fig. 6 shows the constellations for QPSK and 16-QAM signals and Fig. 7 shows the beam pattern. Fig. 6 reveals that the linear imperfections introduced the phase rotation. The dotted line in Fig. 7 representing the beam pattern of the system with linear imperfections shows that the main beam is formed to the wrong direction and the side beams and nulls are formed to the unpredictable directions.

The nonlinearities in the HPA's make matters worse. For simulations, we adopted a traveling wave

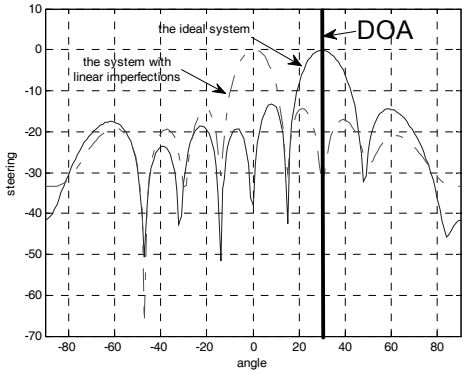

그림 7. 이상적인 시스템과 선형 결함 시스템의 빔 패턴 비교

Fig. 7. Comparison of beam patterns of the ideal system, and the system with linear imperfections.

표 5. 전력 증폭기의 비선형 계수

Table 5. The nonlinear coefficients of the HPA

Amplifier #	The nonlinear coefficient of the HPA
1	$a_a=2,\ \beta_a=1,\ a_p=2.53,\ \beta_a=2.82$
2	$a_a=1.8,\ \beta_a=0.9,\ a_p=2.2,\ \beta_a=2.9$
3	$a_a=2.1,\ \beta_a=1,\ a_p=2.4,\ \beta_a=2.9$
4	$a_a=2,\ \beta_a=1.1,\ a_p=2.5,\ \beta_a=2.8$
5	$a_a=2.2,\ \beta_a=1.1,\ a_p=2.3,\ \beta_a=2.7$
6	$a_a=1.9,\ \beta_a=1.2,\ a_p=2.3,\ \beta_a=2.5$
7	$a_a=1.7,\ \beta_a=0.8,\ a_p=2.6,\ \beta_a=2.6$
8	$a_a=2,\ \beta_a=0.8,\ a_p=2.7,\ \beta_a=2.8$

tube (TWT) amplifier model for the HPA's. The amplitude A and the phase shift Φ of the output signal of the TWT are modeled by the Saleh's model[9] as follows:

$$A[r[n]]=\frac{\alpha_a r[n]}{1+\beta_a r^2[n]} \tag{14}$$

$$\Phi[r[n]]=\frac{\alpha_p r^2[n]}{1+\beta_p r^2[n]} \tag{15}$$

where $\alpha_a, \beta_a, \alpha_p, \beta_p$ are constants and $r[n]$ is the normalized input. In table 5, we show the parameters of the TWT used in this study.

We investigate the system with the linear imperfections and the nonlinearity of the HPA. Fig. 8 shows the constellations for QPSK and 16-QAM signals and Fig. 9 shows the beam pattern of the

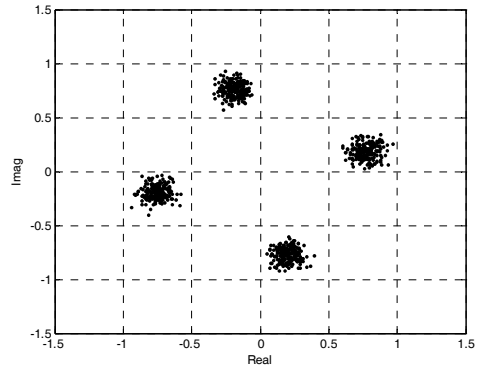

(a) QPSK

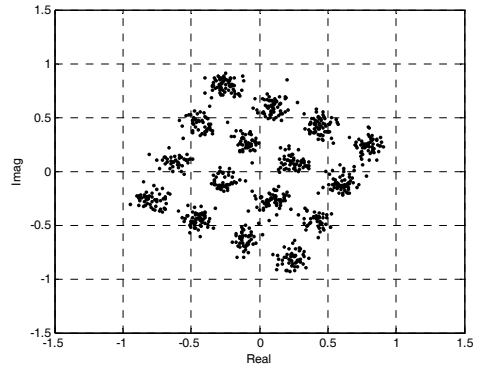

(b) 16-QAM

그림 8. 선형 결함과 비선형 결함을 모두 가진 배열 안테나 시스템의 신호 성상도

Fig. 8. Signal constellations of the antenna array system with both the linear and the nonlinear imperfections.

antenna array without cal-com. Fig. 8 shows that the linear and nonlinear imperfections introduced the constellation miss-alignment as well as the phase rotation. The dotted line in Fig. 9 representing the beam pattern of the system without cal-com shows that the positions of the beams and nulls are formed to the totally wrong directions.

To investigate the effect of the nonlinearity, we attempted to calibrate and compensate with only a linear term. Fig. 10 shows the constellations for QPSK and 16-QAM signals and Fig. 11 shows the beam pattern with the linear term only. Fig. 10 reveals that the linear term alone can not compensate for the constellation blurring resulting from the nonlinearity. Moreover, the dotted line in Fig. 11

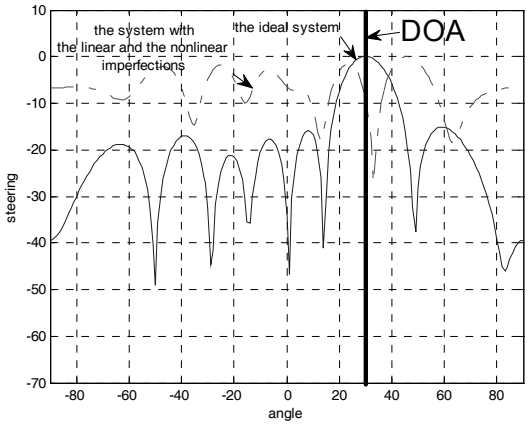

그림 9. 이상적인 시스템과 선형 결함과 비선형 결함이 모두 있는 시스템의 빔 패턴 비교

Fig. 9. Comparison of beam patterns of the ideal system and the system with both the linear and the nonlinear imperfections.

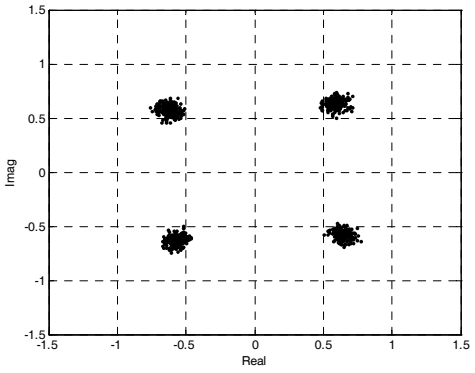

(a) QPSK

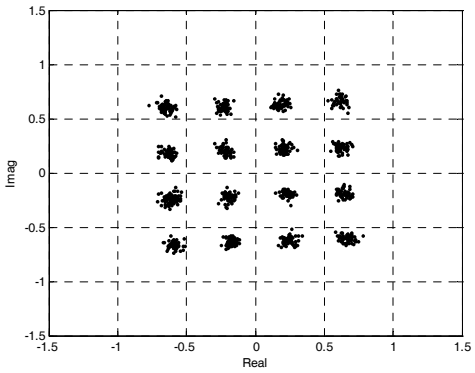

(b) 16-QAM

그림 10. 선형 보정에 의해서만 보정과 보상된 후의 신호 성상도

Fig. 10. Signal constellations after the calibration using a linear term only.

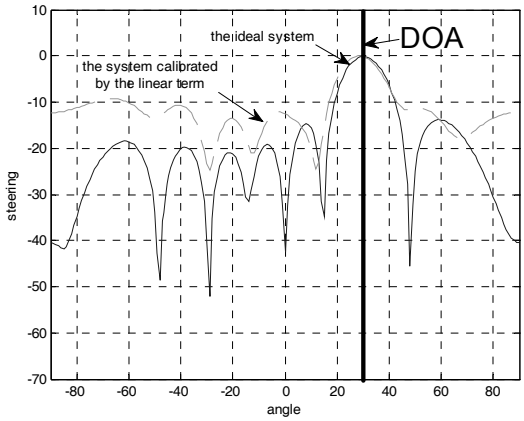

그림 11. 이상적인 시스템과 선형 보정에 의해서만 보정과 보상된 시스템의 빔 패턴 비교

Fig. 11. Comparison of beam patterns of the ideal system and the system calibrated using a linear term only.

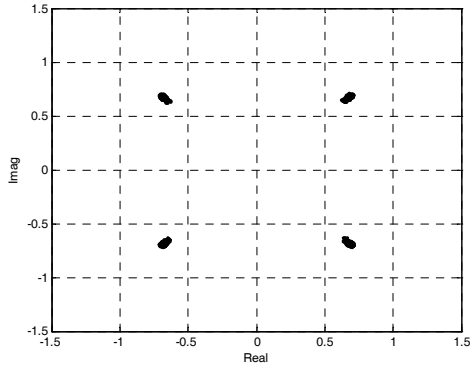

(a) QPSK

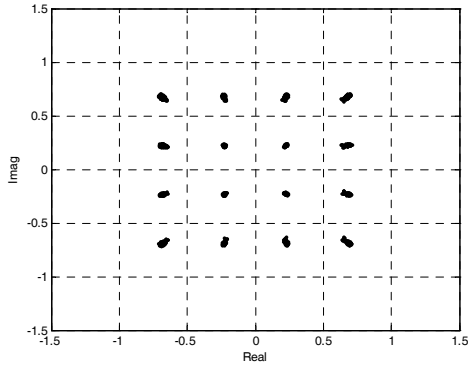

(b) 16-QAM

그림 12. 3차 다항식에 의해 보정과 보상된 후의 신호 성상도

Fig. 12. Signal constellations after cal-com using a third-order polynomial.

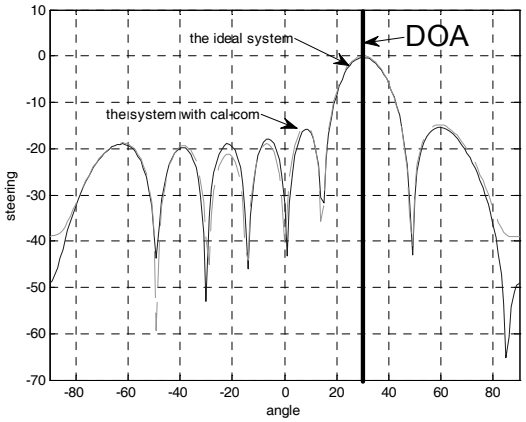

그림 13. 이상적인 시스템과 3차 다항식에 의해 보정과 보상된 시스템의 빔 패턴 비교

Fig. 13. Comparison of beam patterns of the ideal system and the system with cal-com using a third-order polynomial.

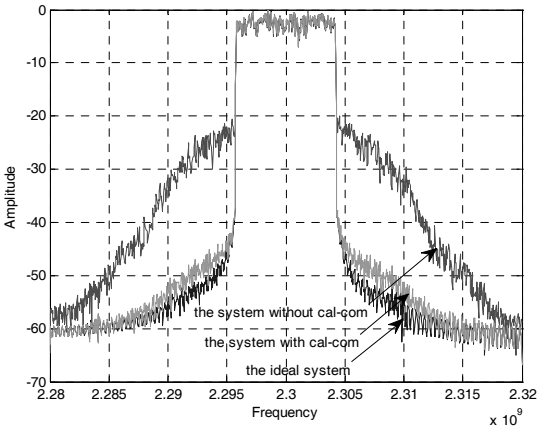

그림 14. 이상적인 시스템, 보정과 보상된 시스템, 그리고 보정과 보상이 없는 시스템의 PSD 비교

Fig. 14. Comparison of PSDs of the ideal system and the systems with and without cal-com.

shows that the main beam is formed to the desired direction, but the side beams and nulls are not formed correctly.

Since the linear and nonlinear imperfections are not effectively calibrated and compensated by the linear term only, we add one third-order nonlinear term to compensate for the nonlinear effects. Fig. 12 shows the constellations for QPSK and 16-QAM signals and Fig. 13 shows the beam pattern with cal-com usingthe linear term plus a third-order term. As Fig. 12 shows, the NMSE (normalized mean- squared

error) of QPSK signals has improved from about -1 dB to about -40 dB, and that of 16QAM signals has improved from -1 dB to about -40 dB. The dotted line in Fig. 13 agrees well with the desired beam pattern.

Finally, we check with the spectral re-growth caused by the nonlinearity. Fig. 14 shows the power spectral densities (PSDs) of the ideal system, and those of the systems with and without the cal-com. With cal-com, we can confirm that the spectral re-growth is suppressed by about 20 dB, which shows that the nonlinear effects are effectively compensated by the added nonlinear term.

Ⅵ. Conclusion

We proposed a new scheme combining the path calibration and the nonlinear HPA compensation in a transmitting antenna array system. We utilized a third-order polynomial for the calibration and compensation and indirect learning architecture for the coefficient updates. We used one common training block for the coefficient updates of all paths by using switching blocks. The result of computer simulations shows that beams and nulls can be formed to thedesired directions even with the efficient HPA's operating near saturation region. The signal quality is recovered as well with a correct constellation and without spectral re-growth. From the results, we can conclude that, with the addition of only one nonlinear term in the calibration, we can not only calibrate the linear imperfections of the antenna array paths but also we can compensate for the HPA nonlinearities, which leads to a linear efficient smart antenna system.

References

[1] Schurhuber Robert, Receiver Imperfections and Calibration of Adaptive Antennas, Ph. D. Thesis, Technischen University at Dresden, 1998.

[2] WU Lili, LIAO Gusheng, ZHANG Linrang, "A blind calibration method for smart antenna system," *Proc. of IEEE Tencon*, Vol. 2, pp. 1031-1034, 2002.

[3] S. Kobayakawa, M. Tsutsui and Y. Tanaka, "A blind calibration method for an adaptive antenna array in DS-CDMA systems using an MMSE algorithm," *Proc. of VTC*, Vol. 1, pp. 21-25, 2000.

[4] M. G. Kyeong, H. G. Park, H. S. Oh and J. H. Jung, "Array calibration for CDMA smart antenna systems," *Journal of ETRI*, Vol. 26, No. 6, pp. 605-614, 2004.

[5] Mattias Wennstrom, Smart Antenna Implementation Issues for Wireless Communications, Ph. D. Thesis, Uppsala University, 1999.

[6] Changsoo Eun and Edward J. Powers, "A New Volterra Predistorter Based on the Indirect Learning Architecture", *IEEE Trans. On Signal Processing*, Vol. 45, No. 1, pp. 223-227, Jan. 1997.

[7] Raymond H. Kwong, Edward W. Johnston, "A Variable Step Size LMS Algorithm", *IEEE Trans. Signal processing*, vol. 40, No. 7, pp. 1633-1642, July 1992.

[8] Simon Haykin, *Adaptive filter theory,* 2nd Ed., Prentice Hall, Inc., pp. 299-359, 1991.

[9] Adel A. M. Saleh, "Frequency-Independent and Freqeuncy-dependent Nonlinear Models of TWT Amplifiers", *IEEE Trans. Commun.*, vol. COM-29, No. 11, pp. 1715-1720, Nov. 1981.

저 자 소 개

임 선 민(정회원)

2000년 충남대학교 정보통신 공학과 학사 졸업.
2002년 충남대학교 정보통신 공학과 석사 졸업.
2010년 충남대학교 정보통신 공학과 박사 졸업.
2006년 8월～현재 한국전자통신연구원 광대역 RF 연구팀.
<주관심분야 : 통신 신호 처리, 이동통신>

은 창 수(평생회원)-교신저자

1985년 서울대학교 전자공학과 학사 졸업.
1987년 서울대학교 전자공학과 석사 졸업.
1995년 텍사스 주립대학 (오스틴) 박사 졸업.
<주관심분야: 통신 신호 처리, RF 회로>

김 민(학생회원)

2005년 충남대학교 전자전자정보 통신공학과 학사 졸업.
2007년 충남대학교 전자전파정보 통신공학과 석사 졸업.
2007년～충남대학교 전자전파정 보통신공학과 박사 과정.
<주관심분야 : 무선 통신, 신호처리>